



**Project Number:** [956004]

**Project Acronym:** [BioTrib]

**Project title:** [Advanced Research Training for the Biotribology of Natural and Artificial Joints in the 21st Century]

## **Tribological properties of bare and gel-infiltrated fibrous materials**

**Deliverable D5.1**

**Month Due: PM30**

**Month Delivered: PM33**

Project coordinator name	Prof. Richard M Hall
Project coordinator organisation name	UNIVLEEDS
Report prepared by	Elisa Bissacco Prof. Stephen J. Ferguson Review by members of the Supervisory Board

### **Dissemination Level of Report**

PU	Public	<input checked="" type="checkbox"/>
PP	Restricted to other program participants (including the Commission Services)	<input type="checkbox"/>
RE	Restricted to a group specified by the consortium (including the Commission Services)	<input type="checkbox"/>
CO	Confidential, only for members of the consortium (including the Commission Services)	<input type="checkbox"/>

The BioTrib ETN project has received funding from the European Union's Horizon 2020 research and innovation programme under grant agreement No. 956004.



Version	Date	Comment	Modifications made by
D5.1.1	19-07-2023	First Draft circulated to SB	Elisa Bissacco
D5.1.2	27-07-2023	Review SB	Stephen Ferguson
D5.1.3	04-08-2023	Review RMH	Richard M Hall
D5.1.3	17-08-2023	Amendment	Elisa Bissacco/Stephen Ferguson
<b>D5.1</b>	<b>06-09-2023</b>	<b>Submitted to Commission</b>	<b>JS (UNIVLEEDS)</b>

## Contents Page

<b><i>Executive Summary</i></b> .....	<b>4</b>
<b><i>Introduction</i></b> .....	<b>5</b>
<b><i>Deliverable Description</i></b> .....	<b>6</b>
<b><i>Materials and Methods</i></b> .....	<b>7</b>
<b><i>Results</i></b> .....	<b>9</b>
<b><i>Discussion</i></b> .....	<b>13</b>
<b><i>Conclusion</i></b> .....	<b>13</b>
<b><i>Bibliography</i></b> .....	<b>14</b>

## Executive Summary

Osteoarthritis (OA) is a prevalent condition affecting millions of adults in the US and is the most common musculoskeletal disorder worldwide [1]. It is characterized by the gradual breakdown of the synovial joints, resulting in pain, stiffness, and reduced functionality. Efforts are being made to develop therapies that improve care, quality of life, and pain relief for OA patients [2].

The limited self-repair capability of damaged cartilage tissue poses a challenge, and various scaffold fabrication technologies have been explored for cartilage engineering [3, 4].

Electrospinning, melt-electrowriting, and gel fabrication have emerged as promising techniques due to their versatility in producing nanofibrous scaffolds with different properties [5]. These advancements hold promise for regenerating damaged cartilage tissue and improving the treatment of osteoarthritis.

The aim of this project is to manufacture chondrocyte-compatible multi-scale electrospun scaffolds from polycaprolactone. Based on previous works, the goal is to obtain good frictional properties utilizing biphasic self-pressurization, which is similar to the mechanisms of natural articular cartilage.

The friction coefficient is expected to directly depend on electrospun material porosity, fiber diameter, chemistry, and orientation. Furthermore, the inclusion of the interstitial gel phase in the scaffold is expected to improve frictional characteristics as well as the fatigue life of the materials.

The objectives of this project will be accomplished through the following steps:

1. Develop and characterize the mechanical properties of electrospun matrices and fiber-reinforced gel scaffold.
2. Develop a poro-viscoelastic FE model of fiber-reinforced gel scaffold.
3. Test chondrocytes' influence on scaffold frictional behavior.
4. Measure time-dependent mechanical and tribological properties.

The technical developments in this project will be broadly applicable in tissue engineering for articular cartilage regeneration. Additionally, this project will lead to new methods in electrospinning and the development of hybrid electrospun gel-infiltrated scaffolds.

This initial scientific deliverable (D5.1) focuses on evaluating the impact of gel introduction on the tribological behaviour of fibrous PCL scaffolds. Contrary to expectations, the pin-on-disc tribological test results revealed that electrospun and melt-electrowritten / electrospun composite scaffolds exhibited a lower coefficient of friction compared to cryogels and fibrous mats embedded in gel. This unexpected result suggests the presence of a lubricant fluid layer between the surface of the non-infiltrated fibrous samples and the countersurface, indicating a full film regime.

## Introduction

Osteoarthritis (OA) affects over 32.5 million US adults and is the most common musculoskeletal condition worldwide. It is also known as degenerative joint disease or “wear and tear” arthritis [1].

OA is a multi-factorial, usually slow progressing, and non-inflammatory disorder of the synovial joints that results from stresses, due to abnormality in any of the synovial joint tissues, including articular cartilage, subchondral bone, ligaments, periarticular muscles, peripheral nerves, or synovium. This leads to the breakdown of cartilage and bone, resulting in pain, stiffness, and functional disability [1]. Due to the significant health, economic, and social problems it causes, strong and cost-intensive efforts have been undertaken to develop therapies to improve care, quality of life, and pain relief for OA patients [2].

Due to the lack of capillary vessels and a very limited self-repair capability, caused by chondrocytes' low metabolic activity, cartilage tissue has a very limited self-repair ability when damaged [6].

Over the years, various scaffold fabrication technologies have been tried out for cartilage engineering with varying levels of success. Among them, electrospinning, melt-electrowriting and gel fabrication have emerged as promising techniques due to their high versatility (e.g., the ability to produce functionalized nanofibrous scaffolds with a variety of orientations, sizes, and mechanical properties) [5].

### a) Solution Electrospinning (SES)

Solution electrospinning (SES) has been used for biomedical applications for a long time. SES is a technique that allows the production of nanofibrous scaffolds and allows for the tuning of the 3D scaffolds by changing the fiber diameter and scaffold porosity. The process consists of a pump that pushes out a polymer solution from a syringe, through a metal needle (spinneret). The presence of a high voltage source that energizes the polymer solution causes the formation of a conical jet (Taylor cone) which is then drawn into a fiber by electrostatic repulsion [7, 8]. The resulting fibers are deposited on a flat or tubular electrode (collector). The thin electrospun fibers range from a few hundred nanometers to a few micrometers and are suitable candidates to mimic the structure of the natural extracellular matrix (ECM) as they can stimulate cell ingrowth and proliferation [9].

### b) Melt-electrowriting (MEW)

In the field of tissue engineering and biofabrication, existing fabrication technologies are being enhanced, and new techniques are emerging [10, 11]. One such recent addition to the group of additive manufacturing technologies is Melt Electrowriting (MEW). Melt Electrowriting combines the advantages of both electrospinning and fused deposition modeling. In this process, a molten polymer is directed toward a collector, which moves relative to the extrusion nozzle, enabling the deposition of polymer fibers at specific positions. The translational movement of the collector applies a mechanical drag force. By precisely controlling the movement of the collector, the polymer fibers can be deposited in a desired location, attracted to the collector, and stabilized by the electrical field [12].

### c) Cryogels

Hydrogels are three-dimensional networks composed of hydrophilic polymers crosslinked either through covalent bonds or through physical intramolecular and intermolecular attractions. Hydrogels can absorb huge amounts of water or biological fluids and swell quickly without dissolving. Due to the

presence of hydrophilic moieties such as carboxyl, amide, amino, and hydroxyl groups, they are characterized by high hydrophilicity. In their swollen state, hydrogels resemble living tissue, as they are in a soft and rubbery state [13, 4].

Cryogels belong to a category of hydrogels that exhibit a macroporous structure with interconnected networks. They are formed by polymerization at extremely low temperatures, resulting in mechanically strong and flexible networks [13]. These unique characteristics make cryogels highly promising as scaffold materials for various biomedical applications. The process of cryogelation involves several steps: phase separation accompanied by the formation of ice crystals, followed by cross-linking and polymerization, and ultimately, the thawing of the ice crystals to create an interconnected and porous cryogel network [14].

#### **d) PCL fibers–gel composites for cartilage tissue engineering**

Electrospinning represents a valid method to produce stochastic or aligned porous fibrous materials that mimic soft tissue's natural collagenous extracellular matrix, thanks to high surface area and good mechanical properties. Melt electrowriting offers increased control over fiber placement with respect to fiber orientation and spacing without the use of any potentially toxic solvents [11]. Cryogels provide a proper three-dimensional environment and can be loaded with biological agents such as growth factors. They are also able to mimic the proteoglycan-based ground substance of tissue ECM [6, 14]. Furthermore, due to their cartilage tissue-like features, developing hydrogels is now a focus of research to treat cartilage defects [4, 15].

However, these types of scaffolds each have some functional limitations. Cryogels' mechanical properties do not closely resemble those of articular cartilage. On the other hand, electrospun scaffolds, mainly due to low porosity, lead to restricted cell infiltration [6, 14]. Furthermore, for the fabrication of highly porous scaffolds with a small fiber distance with MEW, intrinsic process limitations must be considered. These limitations arise from the electrostatic forces between the fibers being deposited, necessitating a minimum distance between adjacent fibers to avoid printing defects [16].

Several research groups have recently developed composite scaffolds by combining synthetic polymer-based electrospun fibers with natural polymer-based hydrogels, or polymer-based electrospun fibers with melt-electrowritten substrates [17]. Nevertheless, there is still limited literature and knowledge on combining electrospun nanofibers with MEW substrates and incorporating them in hydrogel scaffolds [14]. Thus, the fabrication of such constructs is innovative and novel [6, 14].

### **Deliverable Description**

Natural soft tissues, such as cartilage, have exceptional frictional qualities due to their fiber-reinforced hydrated structure, to the resulting mechanism of biphasic self-pressurization, and to the delayed fluid expression under stress.

In this study, our objective is to design and mechanically and morphologically characterize a biomimetic hybrid scaffold. This scaffold is comprised of electrospun and melt-electrowritten polycaprolactone (PCL) nano- and microfibers surrounded by a microporous gelatine/chitosan cryogel, serving as a framework for supporting the growth of new cartilage tissue. It is created by incorporating novel engineering and biological techniques. By comparing the properties of the hybrid scaffold with the

individual materials, used in its composition, in their original state, our aim is to evaluate its performance.

## Materials and Methods

### Fabrication of PCL nano- and microfiber Scaffolds, Gelatin/Chitosan Cryogel, and Hybrid Scaffold.

For the electrospun fiber scaffold (EF), PCL (Sigma-Aldrich, 440744,  $M_n = 80000 \text{ g mol}^{-1}$ ) was dissolved for 24 h under constant stirring at 11% (w/v) in  $\text{CH}_3\text{OH}:\text{CHCl}_3 + 0.04 \%$  NaCl. Electrospinning was performed by using an electrospinning machine (EC-CLI, IME Technologies, ETH Zürich) for 120 min under the following conditions: flow rate =  $1.62 \text{ mL h}^{-1}$ , electric potential of the nozzle = 16 kV, electric potential of the collector =  $-1 \text{ kV}$ , size of needle = 20G, flat collector, and distance between nozzle and collector = 20 cm (Figure 1). Electrospun fibers were collected onto a glass substrate on top of the flat collector.

After spinning, samples were cut into cylinders with a  $\phi 7 \text{ mm}$  biopsy punch. The average EF specimen thickness was 0.4 mm.

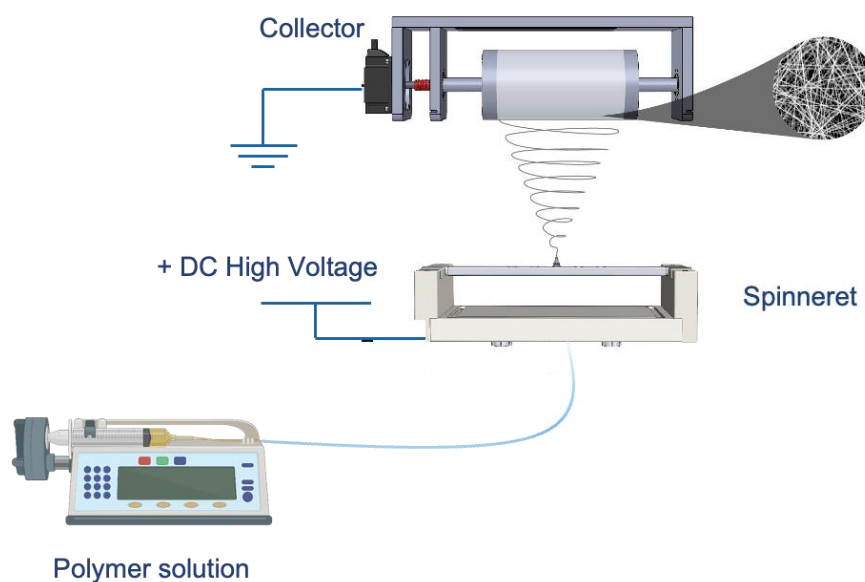


Image Credit: Inovenso

Figure 1: Schematic representation of an electrospinning device.

To fabricate a combined scaffold using EF (Electrospun Fibers) and melt-electrowritten (EMF) membranes, the melt electrowriting (MEW) technique was employed (Figure 2). MEW was performed on EF utilizing a specially constructed melt electrowriting device designed by Matthias Santschi (Laboratory of Orthopaedic Technology, ETH Zürich). The device consists of a vertically moving melt head and a horizontally translating collector. The polymer material in the melt head was maintained in a 5 mL syringe (Braun, Melsungen, Germany) connected to a 22 G blunt needle (Nordson, Westlake, OH, USA). To keep the polymer molten, a heating jacket was employed. Air pressure was applied to extrude the molten polymer through the needle. The collector was composed of a detachable soda-lime glass plate, 1 mm thick, on which the EF matrix was previously deposited, on top of an aluminum plate.

Negative pressure was applied between the glass and aluminum plates to ensure their attachment. High voltage, both positive and negative, was applied to the needle and aluminum plate, respectively. The printing process was controlled using Mach4 software (Version 4.2.0.4612, Newfangled Solutions, Livermore Falls, ME, USA), commonly utilized for CNC machines. Temperature and relative humidity were regulated using a climate control chamber (Parameter, Black Mountain, NC, USA). To generate the motion commands for the device, a custom Python tool was developed to generate G-codes. This allowed for the production of scaffolds with predetermined architectures.

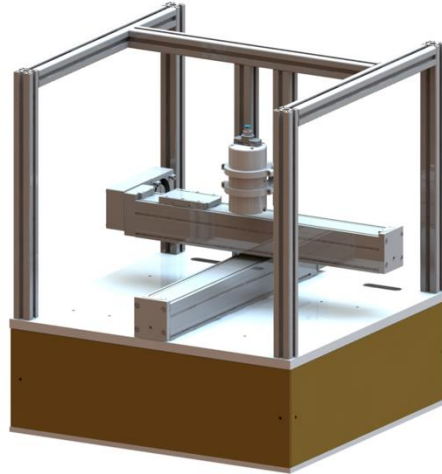


Figure 2: Schematic representation of the melt-electrowriting device. Adapted from Alessio Amicone (ESR2).

For gelatin/chitosan cryogel (GC), chitosan (Sigma-Aldrich, 448869) and type A gelatin (Sigma-Aldrich, G2500) were dissolved in 1% acetic acid solution (Merck, 100063) at a final concentration of 1.5% (w/v) gelatin and 0.6% (w/v) chitosan. 1% (w/v) glutaraldehyde (Sigma-Aldrich, 340855) was used as the crosslinker of GC, and the required 1% glutaraldehyde volume for GC was one-fourth of mixed gelatin/chitosan solution. After mixing all the components, 125  $\mu\text{L}$  of the precursor solution was put in a pre-cooled cylindrical cryogel mold ( $d$  7 mm,  $h$  2 mm) and placed at  $-20$  °C refrigerator for overnight cryogelation.

For hybrid scaffolds (EF-GC, EMF-GC) composed of EF and GC and of EMF and GC, EF and EMF scaffolds that were first treated with NaOH (1 M) for 4 hours, washed with  $\text{dH}_2\text{O}$  three times, soaked in  $\text{dH}_2\text{O}$  overnight, and consequently freeze-dried. The membranes were then presoaked for 24h with GC. Finally, after 25  $\mu\text{L}$  of GC solution was pipetted into precooled cylindrical molds, the scaffolds were added to the solution, ensuring a smooth connection between the GC solution and EF and EMF. Then, another 100  $\mu\text{L}$  of GC solution was pipetted to keep EF and EMF scaffolds covered with GC solution. After pipetting, the molds were placed in a  $-20$  °C refrigerator for overnight cryogelation. After cryogelation, scaffolds were lyophilized to remove ice crystals.

## Characterization of electrospun scaffold

### Tribological tests

All sample types underwent clockwise circular friction tests. Six replicates were used per type of sample. Specimens were cut in 7 mm diameter cylinders, glued with dual epoxy to 3D printed (CREATBOT PEEK 300, LTU Luleå) PLA supports and soaked in PBS for 24h. Samples were then mounted on the pin holder and secured vertically on the machine. The friction test was conducted using a CETR UMT Test



System pin-on-disc apparatus. The tests were controlled by a custom software (UMT – CETR, LTU Luleå). A cobalt chromium disc with a diameter of 20 mm served as the counterface material. Throughout the test, PBS was applied as a lubricant.

Prior to commencing the test, a preload of 0.5 N was applied for a duration of 30 seconds. Following the preload, the test was initiated by applying a load of 1 N (corresponding to 0.026 MPa) to the 7 mm diameter pin. The pin was placed 15 mm from the centre of the disc, that was then subjected to a rotating velocity of 4.8 rpm for a resulting reciprocal velocity of 7.5 mm/s.

The entire test was conducted at a temperature of 25°C.

Additional tests were run in dry conditions, applying the same parameters.

### Scanning Electron Microscopy

The morphology and microstructure of EF, EMF and lyophilized GC, EF-GC, and EMF-GC scaffolds were observed by scanning electron microscopy (Jeol JSM-IT300, LTU Luleå).

Samples were lyophilized and coated with platinum sputtering (Leica EM ACE200, LTU Luleå). Images were analysed with ImageJ software (NIH, United States) to analyse the average fiber diameter of the EF and EMF samples.

### Statistics

All experiments were performed with six replicates, and all data were analysed as mean  $\pm$  SD. For statistical analysis, one-way ANOVA was performed, and statistical significance was defined as a  $p$ -value:  $p < 0.05$  (\*),  $p < 0.01$  (\*\*),  $p < 0.001$  (\*\*\*),  $p < 0.0001$  (\*\*\*\*).

## Results

### Tribological test

The experimental results for the friction coefficient in the pin on disc testing are shown in Figure 3. The friction coefficient was substantially higher for GC, EF-GC and EMF-GC samples, compared to non-infiltrated EF and EMF samples (Figure 4).

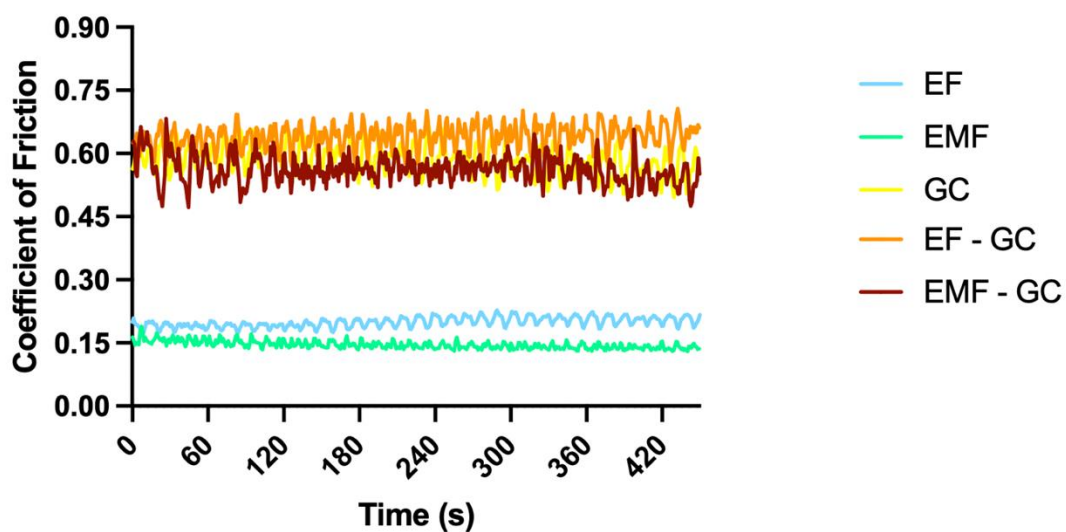


Figure 3: Graph showing average friction coefficient (over six replicates) of different scaffold types.

In general, the EMF scaffolds showed the lowest coefficient of friction among all the specimens, whilst EF-GC showed the highest value.

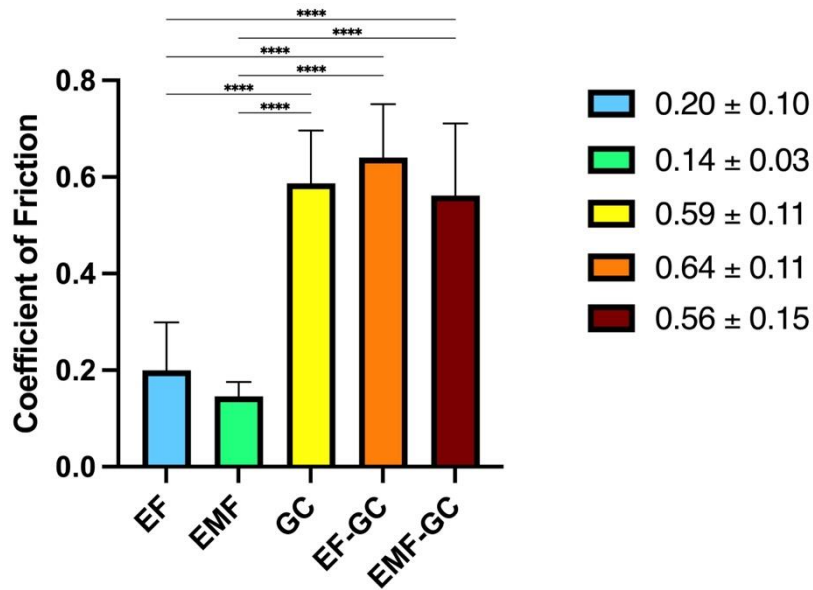


Figure 4: Friction coefficient values of different scaffold types in wet conditions.

The dry test showed quite a different outcome (Figure 5).

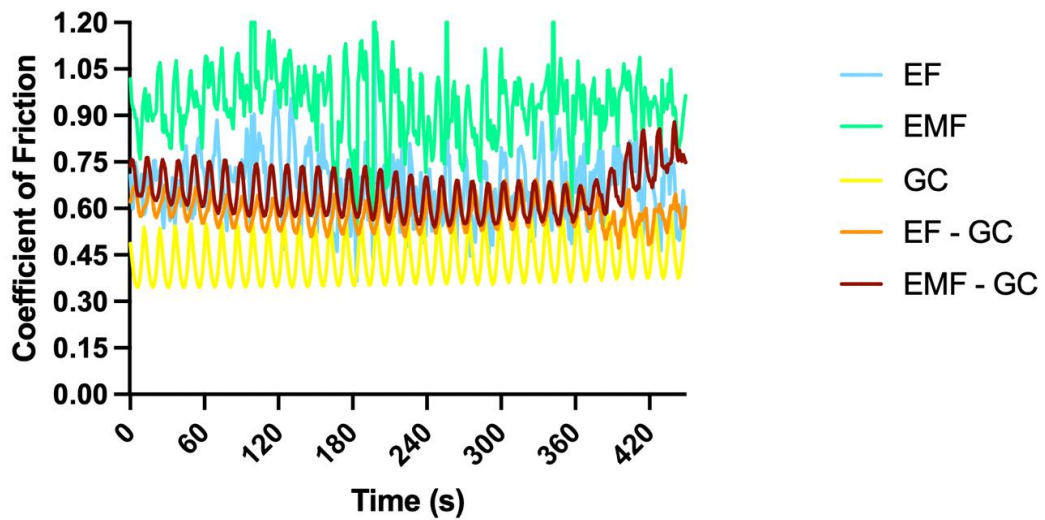


Figure 5: Graph showing average friction coefficient (over six replicates) of different scaffold types.

In dry conditions, EMF scaffolds showed the highest coefficient of friction among all the specimens, whilst GC showed the lowest value (Figure 6).

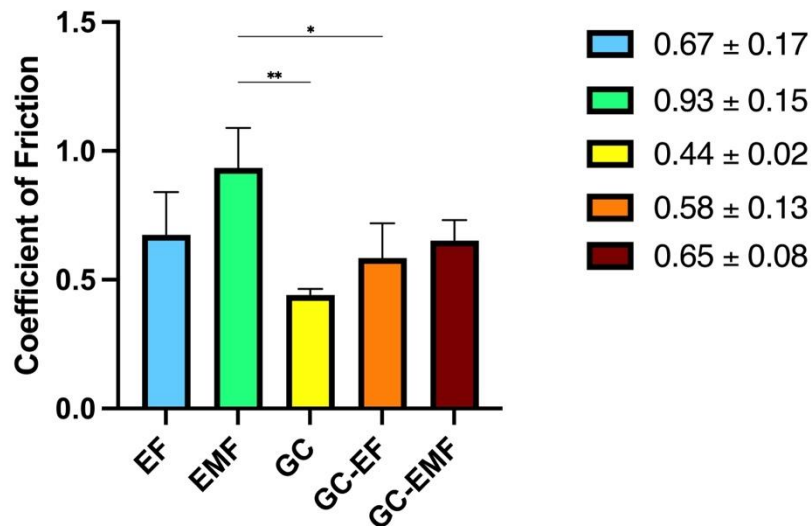


Figure 6: Friction coefficient values of different scaffold types in dry condition.

### Scanning Electron Microscopy

We used SEM to characterize the sample surfaces and structure before and after the friction experiment. Figure 8 shows the surface fibers of EF (A, C) and EMF (B, D) scaffolds before and after undergoing the frictional test.

For both EF and EMF samples, the fiber diameters increased significantly after the test (Figure 7).

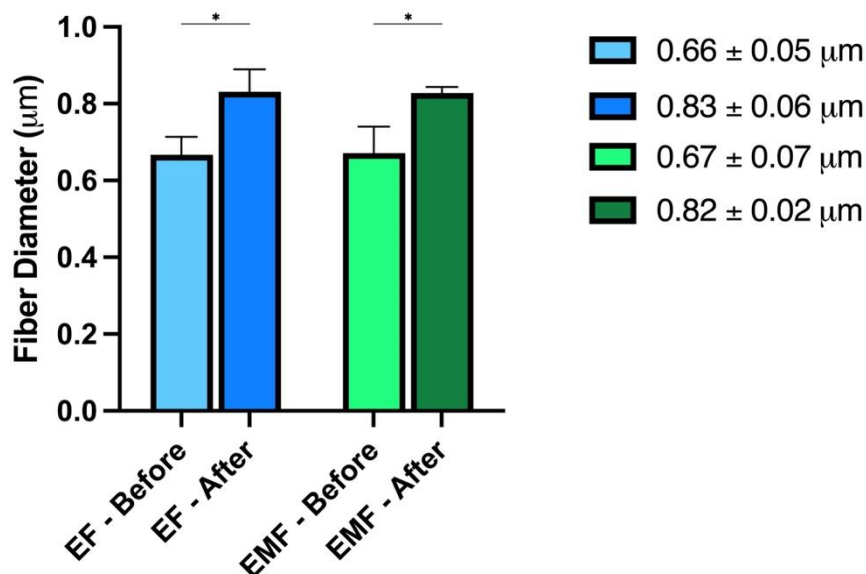


Figure 7: Fiber diameters of EF and EMF before and after pin on disc tests.

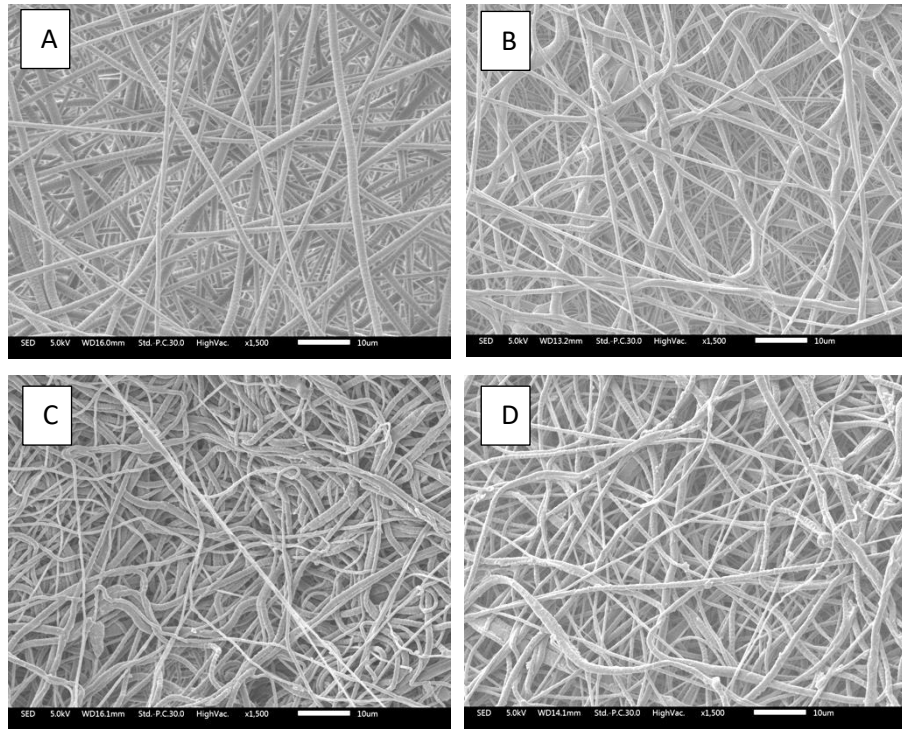


Figure 8: SEM images of EF and EMF before (A, B) and after (C, D) frictional tests.

For the cryogels (GC), our analysis of SEM images revealed a qualitative increase in surface roughness when comparing the samples before and after testing (Figure 9A, 9D). Specifically, in the case of EF-CG and EMF-CG, the surface of the post-test samples exhibited a more prominent appearance of the underlying fiber matrix (Figure 9E, 9F).

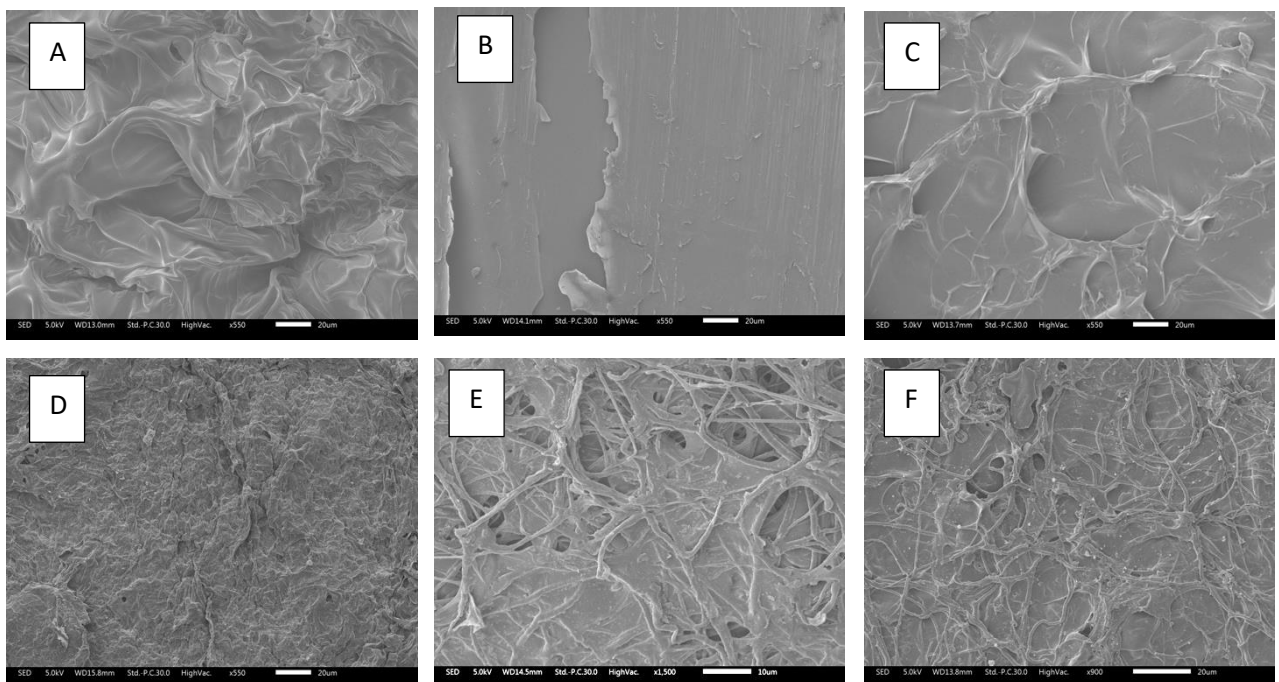


Figure 9: SEM images of GC, EF-GC and EMF-GC before (A, B, C) and after (D, E, F) frictional tests.

## Discussion

Contrary to expectations, the pin-on-disc tribological test results revealed that EF and EMF exhibited a lower coefficient of friction compared to cryogels and fibrous mats embedded in gel. This unexpected result suggests the presence of a lubricant fluid layer partly supporting the load between the surface of the EF and EMF samples and the countersurface, indicating a mixed lubrication regime. This is further supported by the higher friction coefficient observed in the dry conditions for the fibrous matrices, indicating the absence of a fluid layer between the pins and countersurface.

On the other hand, the higher coefficient of friction observed in CG, EF-CG, and EMF-CG can be attributed to the semi-adhesive properties typically associated with materials like chitosan and porcine gelatine [18]. This may explain the apparent deterioration of scaffold frictional properties observed in cryogel scaffolds, which exhibit a coefficient of friction outside the range of native articular cartilage [19].

The combination of EF with EMF demonstrates an improvement in the frictional properties of the scaffolds, possibly due to water retention within the pores of the melt-electrowritten matrix. SEM images revealed an increased mean fiber diameter in both EF and EMF samples after the frictional tests, likely due to the applied contact pressure on the samples.

The higher noticeable roughness observed in CG can be attributed to the direct frictional contact between the sample surface and the metal disc countersurface, without an interposed fluid film. This may also explain the more visible fibrous matrix on the surface of CG-EF and CG-EMF samples, possibly resulting from the removal of the superficial layer of cryogel that initially covered the fibrous matrices.

## Conclusion

In conclusion, our study demonstrates that the inclusion of a gel phase in the matrix scaffolds alters the frictional behavior of the samples. Moreover, we observed that the combination of a melt-electrowritten matrix with an electrospun matrix, with or without the presence of cryogel, contributes to an improved frictional response of the scaffold. These findings hold promise for our goal of developing a multi-scale fibrous scaffold for articular cartilage regeneration.

However, further investigations and solutions regarding the role of the gel phase are necessary. It may be beneficial to make slight modifications to the composition of the gel phase or its distribution within the scaffold architecture in order to optimize the results.

## Bibliography

- [1] N. Lane, K. Brandt, G. Hawker, E. Peeva, E. Schreyer, W. Tsuj and M. Hochberg, "OARSI-FDA initiative: defining the disease state of osteoarthritis," *Osteoarthritis and Cartilage*, pp. 478 - 482, 2011.
- [2] S. Grässel and D. Muschter, "Recent advances in the treatment of osteoarthritis," *F1000Research*, vol. 9, 2020.
- [3] C. Vinatier and J. Guicheux, "Cartilage tissue engineering: From biomaterials and stem cells to osteoarthritis treatments," *Annals of Physical and Rehabilitation Medicine*, vol. 59, pp. 139 - 144, 2016.
- [4] W. Wei, Y. Maa, X. Yao, W. Zhou, X. Wang, L. Chenglin, J. Lin, Q. He, S. Leptihna and H. Ouyang, "Advanced hydrogels for the repair of cartilage defects and regeneration," *Bioactive Materials*, vol. 6, p. 998–1011, 2013.
- [5] E. Yilmaz and D. Zeugolis, "Electrospun Polymers in Cartilage Engineering — State of Play," *Frontiers in Bioengineering and Biotechnology*, vol. 8, 2020.
- [6] H. Lin, W. Tsai and S. Chang, "Collagen-PVA aligned nanofiber on collagen sponge as bi-layered scaffold for surface cartilage repair," *Journal of Biomaterials Science*, vol. 28, 2017.
- [7] N. Maurmann, L. Sperling and P. Pranke, "Electrospun and Electrospayed Scaffolds for Tissue Engineering," *Cutting-Edge Enabling Technologies for Regenerative Medicine*, pp. 79 - 100, 2018.
- [8] R. Soares and al., "Electrospinning and electrospray of bio-based and natural polymers for biomaterials development," *Mater Sci Eng C Mater Biol Appl*, pp. 969-982, 2018.
- [9] D. Alexeev and al., "Electrospun biodegradable poly(epsilon-caprolactone) membranes for annulus fibrosus repair: Long-term material stability and mechanical competence," *JOR Spine*, vol. 1, 2021.
- [10] J. Meng and al, "Design and manufacturing of 3D high-precision micro-fibrous poly (l-lactic acid) scaffold using melt electrowriting technique for bone tissue engineering.," *Materials & Design*, vol. 210, 2021.
- [11] M. Castilho and al., "Melt electrowriting allows tailored microstructural and mechanical design of scaffolds to advance functional human myocardial tissue formation.," *Advanced Functional Materials*, vol. 28(40), 2018.
- [12] A. Dufour and al., "Integrating melt electrowriting and inkjet bioprinting for engineering structurally organized articular cartilage.," *Biomaterials*, vol. 283, 2022.

- [13] I. El-Sherbiny and M. Yacoub, "Hydrogel scaffolds for tissue engineering: Progress and challenges," *Global Cardiology Science and Practice*, vol. 38, 2013.
- [14] A. Semitela, A. Girão, C. Fernandes, G. Ramalho, I. Bdikin, A. Completo and P. Marque, "Electrospinning of bioactive polycaprolactone-gelatin nanofibres with increased pore size for cartilage tissue engineering applications," *Journal of Biomaterials Applications*, vol. 35, p. 471–484, 2020.
- [15] L. Han, K. Liu, M. Wang, K. Wang, L. Fang, H. Chen and al, "Mussel-inspired adhesive and conductive hydrogel with long-lasting moisture and extreme temperature tolerance," *Adv. Funct. Mater.*, vol. 18, 2018.
- [16] S. Loewner and e. al., "Recent advances in melt electro writing for tissue engineering for 3D printing of microporous scaffolds for tissue engineering," *Frontiers in Bioengineering and Biotechnology*, 2022.
- [17] S. Lee, M. Santschi and S. Ferguson, "A Biomimetic Macroporous Hybrid Scaffold with Sustained Drug Delivery for Enhanced Bone Regeneration," *Biomacromolecules*, vol. 22, p. 2460–2471, 2021.
- [18] Y. Mosleh, W. Zeeuw, M. Nijemeisland and a. al., "The Structure–Property Correlations in Dry Gelatin Adhesive Films," *Adv. Eng. Mater.* , vol. 23, 2021.
- [19] S. Oungouljian, K. Durney, B. Jones, C. Ahmad, Hung and A. GA, "Wear and damage of articular cartilage with friction against orthopedic implant materials. J Biomech.," *J Biomech*, 2015.